Multidisciplinary Journal of Chemistry
Volume 11 Issue 1, January-March 2023
ISSN: 2995-4398
Impact Factor: 7.15
https://kloverjournals.org/journals/index.php/chem

MAGNETITE MAGIC: INVESTIGATING THE IMPACT OF U. TOMENTOSA LEAF-EXTRACTED NANOPARTICLES ON GREEN PEACH APHID INFESTATION

Dr. Salma Nour Abdallah
Department of Plant Protection, School of Agriculture, The University of Jordan, Amman 11942, Jordan.

Abstract
Magnetite (Fe_3O_4) nanoparticles have gained significant attention due to their diverse applications in various fields, including biomedicine, agriculture, and diagnostics. The tunable properties of these nanoparticles make them suitable for targeted drug delivery, cancer diagnostics, magnetic resonance imaging, catalysts, pharmaceuticals, and more. Several synthesis methods have been developed to prepare magnetite nanoparticles, but many of these methods involve purification steps, hazardous by-products, and high-temperature conditions. In response to these limitations, researchers have turned to environmentally friendly and cost-effective "green" synthesis routes using plant extracts.
In this study, we explored the synthesis of magnetite nanoparticles (Fe_3O_4NPs) through a green approach, utilizing the aqueous extract of Urtica tomentosa leaves. This method provides an eco-friendly, cost-effective, and non-toxic alternative to traditional synthesis routes. The magnetite nanoparticles obtained through this green synthesis route were characterized for their potential impact on green peach aphids.
The use of magnetite nanoparticles in pest control is a novel and innovative approach. These nanoparticles have shown promise in various applications, but their effects on pests like green peach aphids remain relatively unexplored. The current study addresses this gap by investigating the influence of Fe_3O_4NPs on green peach aphid populations.

Keywords: Magnetite nanoparticles, green synthesis, Urtica tomentosa, green peach aphid, eco-friendly nanoparticles.

1. Introduction

Magnetite (Fe_3O_4) is magnetic iron oxide encountered in many biological and technological applications. The particle size and shape of magnetite nanoparticles allows tuning their properties to different applications such as targeted drug delivery, cancer diagnostic, magnetic resonance imaging, catalysts, pharmaceuticals, biomedicine, and agriculture. Various routes and methods have been developed for synthesis magnetite nanoparticles (Fe_3O_4NPs) such as co-precipitation method (Petcharoen and Sirivat, 2012), solvothermal reduction method (Hou et al., 2003, Ou et al., 2010), thermal decomposition method (Chin et al., 2011, Angermann and Töpfer, 2008), electrochemical synthesis (Cabrera and Gutierrez, 2008), sol-gel method (Xu et al., 2007), W/O micro-emulsion (Lu et al., 2004), via a solventfree thermal decomposition route (Maity et al., 2009), hydrothermal synthesis

(Ge et al., 2009, Iwasaki et al., 2012), polyol method (Vega-Chacón et al., 2016), high temperature phase reaction of iron acetate in phenyl ether with alcohol (Sun and Zeng, 2002) and by high energy ball milling (de Carvalho et al., 2013). All these methods and routes of synthesis require extra purification steps, reaction times, hazardous by-products, high temperature and difficulty of scale-up, therefore researchers concentrated on the green routes for synthesis magnetite nanoparticles (Fe3O4NPs) due to an eco-friendly, cost-effective and non-toxic routes by using plant extracts such as carob leaf extract (Awwad and Salem, 2012), Pistachio leaf extract (Salem et al., 2013), *Kappaphycus alvarezii* extract (Yew et al., 2016), *Sargassum muticum* aqueous extract (Mahdavi et al., 2013), *Dhatura innoxia* plant extract (Das et al., 2014), *Caricaya Papaya* Leaves (Latha1 and Gowri, 2014), *Azadirachta indica* leaf extract (Maheswari and Reddy, 2016), *Tridax procumbens* leaf extract (Senthil and Ramesh, 2012), *Averrhoa carambola* (Ahmed et al., 2015), *Jatropha gosspifolia* leaves (Karkuzhali and Yogamoorthi, 2015), and *hordeum vulgare* and *Rumexacetosa* plants (Valentin et al., 2014).

This research workwas carried out to study the effect of magnetite (Fe3O4NPs) nanoparticles on green peach aphid. A facile, eco-friendly and green route was used for synthesis magnetite nanoparticles using *U. tomentosa* leaf aqueous extract.

2. Experimental 2. 1. Materials

Ferrous chloride (FeCl2.4H2O, 98%) and ferric chloride (FeCl3, 99.99%) were supplied by Sigma-Aldrich. Deionized water was used in all experimental work. *U. tomentosa* is a liana deriving its name from hook-like thorns that resemble the claws of a cat. *U. tomentosa* can grow to a length of up to 30 m, climbing by means of these thorns. The leaves are elliptic with a smooth edge, and grow in opposing pairs. Cat's claw leaves were collected from the campus of Royal Scientific Society, Amman, Jordan.

2.2. Plant aqueous extract of Uncaria tomentosa

U. tomentosa leaves,

Figure 1 were washed several times by water to remove dust and left to dry for two weeks at room temperature in our laboratory. Afterwards, dried leaves were crushed and ground to give fine powder. 20g of leaves powder of *U. tomentosa* were boiled in 500ml de-ionized water for 10min and then filtered on Whatmann filter paper to obtain an aqueous yellow extract. The aqueous extract was kept in tight glass bottle for further experimental work,

Multidisciplinary Journal of Chemistry
Volume 11 Issue 1, January-March 2023
ISSN: 2995-4398
Impact Factor: 7.15
https://kloverjournals.org/journals/index.php/chem

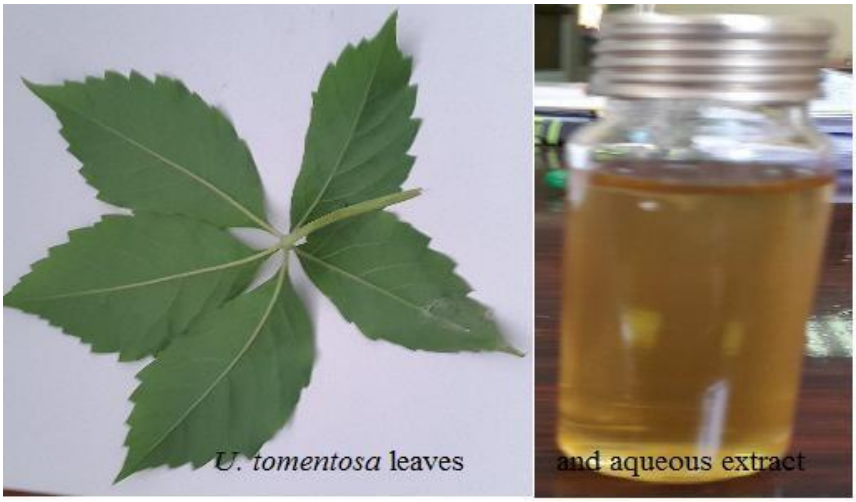

Figure 1. U.tomentosa leaves and aqueous e4xtract

2.3. Green synthesis of magnetite nanoparticles (Fe3O4NPs)

2.3.1. Synthesis from ferrous chloride (FeCl2.4H2O) prucessors

In a typical reaction, 1.2g of FeCl2 was dissolved in 400ml de-ionized water under continuous stirring at room temperature (270C). Afterwards, *U. tomentosa* aqueous extract is added drop by drop, the pale brown color of ferrous chloride solution changed very fast to deep brown color and then to dark color with 2 min. Ratio of FeCl2 solution to the aqueous extract of *U. tomentsa* was 40:1. For analysis, the obtained magnetite nanoparticles were washed three times with de-ionized water and with ethanol to obtain magnetite nanoparticles powder for XRD, SEM, TEM, FT-IR analysis.

2.3.2. Synthesis from ferrous chloride (FeCl2.4H2O) and ferric chloride (FeCl3) prucessors

In a typical reaction, 1.6g ferric chloride (FeCl3) was dissolved in 400ml de-ionized water under continuous stirring at room temperature (270C). Afterwards, 10ml of aqueous extract of *U. tomentsa* is added drop by drop to ferric chloride solution, Color of the mixture FeCl3/*U.tomentsa* changed to deep brown color. Then 0.8g FeCl2 /100ml de-ionized water solution is added drop by drop to the mixture of FeCl3/*U.tomentsa*, very fast changed in the color of the mixture within 1min to grey-black color indicating the formation of magnetite nanoparticles.

2.4. Characterization techniques

Magnetite nanoparticles were characterized by different techniques: UV-vis spectroscopy (Shimadzu UV1601), X-ray diffraction (XRD-6000), fourier transform infrared (FT-IR, IR-Prestige-21 Shimaduz), and transmission electron microscopy (TEM, Hitachi 7600 machine).

2.5. Aphicidal effect of synthesized (Fe3O4NPs) on the green peach aphid (GPA)

2.5.1. GPA culture preparation and rearing:

Two cultures of the GPA were prepared. Pure culture of the GPA from infesting pepper plant by adults of the GPA was collected from Ghor al Safi (Jordan) reared under greenhouse conditions in the University of Jordan and considered as a source culture for all experiments of the study. Another culture was on green pepper plants in the growth chamber under lab conditions at Shouback center for

agricultural research and extension (20-24oC and 16L:8D photoperiod) to get high population of the GPA. New pepper transplants were provided as needed for both cultures. To avoid resistance, GPA was reared for 10 generations on pepper plant before used in the study.

2.5.2 Toxicity of green synthesized magnetite (Fe3O4)NPson the GPA:

Different concentrations of Fe3O4NPs were prepared in 100 ml final volume. Dipping method in which infested leaves of the pepper plants by GPA (50- 60 apterous aphid individual/leaves) were used. Leaf disks were dipped in each concentration for 5 sec then placed in 9 cm Petri dishes having wetted filter paper. Petri dish covered by led with ventilation holes were placed under lab conditions (16 L: 8 D) period and 20-25oC. Each concentration was represented by 6 replicates. Individuals of the GPA were grouped in two groups represented 1st and 2ednymphal instar named early instars as group one and 3ed and 4thnymphal instar named late instars as the other group. Mortality percent was calculated for 24h, 48h and 72h after the treatment. Fine brush was used to assess mortality under dissecting binocular microscope. Mortality assessment was based on lack of antenna and/ or leg movements

3. Results and discussion

3.1. UV-vis spectroscopic analysis

Magnetite nanoparticles synthesized by *U. tomentosa* leaves aqueous extract, which acts as oxidizing and stabilizing agent was monitored by the UV-vis spectrophotometer, An absorbance spectrum, **Figure 2** was observed in each spectrum at 238nm which is characteristic of magnetite nanoparticles. No other peaks were observed in the spectrum, indicating the high purity of the synthesized magnetite nanoparticles by this fast and green method.

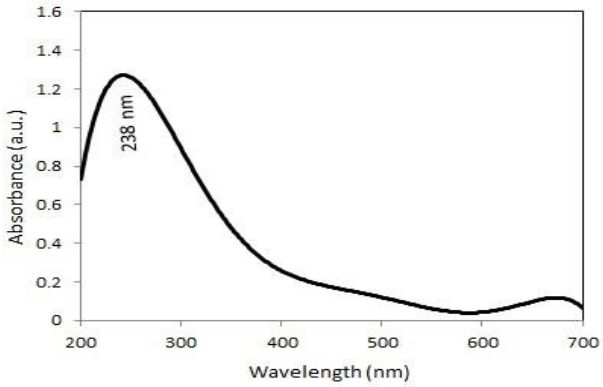

Figure 2. UV-vis spectrum of synthesized magnetite nanoparticles

3.2. X-ray diffraction (XRD) analysis

XRD pattern showed numbers of Bragg's reflections that may be indexed on the basis of the face cantered cubic structure of magnetite. A comparison of XRD spectrum of synthesized magnetite nanoparticles (Fe3O4NPS) with the standard XRD data for bulk magnetite (JCPDS file No. 19-0629) confirmed that the magnetite particles formed in our experiments were in the form of nanocrystals, as evidenced by the peaks at 2θ values of 18.430, 30.770, 36.420,43.480, 54.550, 56.780 and 62.280 corresponding to (111), (220), (311), (222), (400), (422) and (511) Bragg's reflections, respectively, **Figure 3**, which may be indexed based on the face centered cubic (fcc) structures of magnetite. The X-

Multidisciplinary Journal of Chemistry
Volume 11 Issue 1, January-March 2023
ISSN: 2995-4398
Impact Factor: 7.15
https://kloverjournals.org/journals/index.php/chem

ray diffraction results clearly show that the magnetite nanoparticles formed by our green method in presence of *U. tomsentos* leaf extract are crystalline in nature.

It was found that the average size from XRD data and using Debye-Scherer equation was approximately 12 nm. The presence of structural peaks in XRD patterns and average crystalline size around 12 nm clearly illustrates that magnetite particles synthesized by our green method were nano-crystalline in nature. The average particle size of magnetite nanoparticles calculated using Debye-Scherrer equation (Salem et al., **2**013): $D = K\lambda/\beta \cos\theta$

Where D is the mean diameter of nanoparticles, β is the full width at half-maximum value of XRD diffraction lines, λ is the wavelength of X-ray radiation source 0.15405 nm, θ is the half diffraction angle –Bragg angle and K is the Scherrer constant with value from 0.9 to 1. The presence of structural peaks in XRD patterns and average crystalline size calculated 12 nm clearly illustrates the magnetite synthesized were nanocrystalline in nature.

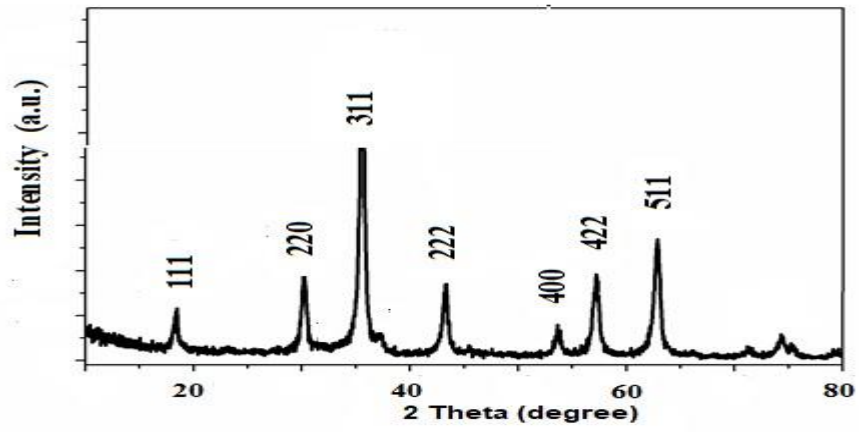

Figure 3. XRD pattern of synthesized magnetite nanoparticles

3.3. Fourier transforms infrared spectroscopy analysis

FT-IR spectra of *U. tomensota* leaves extract is shown in **Figure 4.** The *U. tomensota* leaves extract displays a number of absorption peaks, reflecting its complex nature. Peak at 3383 cm–1 results are due to the stretching of -OH groups of alcohol and phenol compounds. The strong absorption peaks at 2924 cm–1 and 2850 cm-1 could be assigned to –CH stretching vibrations of –CH3 and –CH2 functional groups in aliphatic and aromatic compounds. The shoulder peak at 1739 cm–1 and strong peak at 1612 cm-1 indicated the fingerprint region of C=O and N–H groups in amide (I) and amide (II) of protein. The intense band at 1442 cm-1 and 1230 cm-1 can be assigned to the C-N stretching vibrations of aliphatic amines. The peak at 1064 cm-1 may be attributed to C-O-C stretching mode of aromatic ether linkage group. The peak at 621 cm-1 indicates the –OH bending of the phenolic groups. FTIR study indicated that the free hydroxyl (-OH), carboxyl (-C=O), C-N and amine (N- H) groups present in the structure of *U. tomensota* leaves extract are mainly involved directly in synthesis of magnetite nanoparticles, **Figure 5.**

Multidisciplinary Journal of Chemistry
Volume 11 Issue 1, January-March 2023
ISSN: 2995-4398
Impact Factor: 7.15
https://kloverjournals.org/journals/index.php/chem

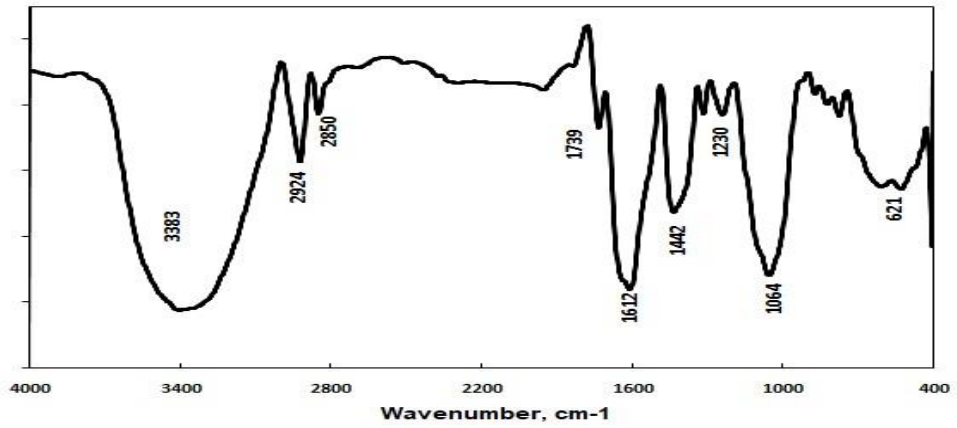

Figure 4. FT-IR spectrum of U. tomensota leaves extract

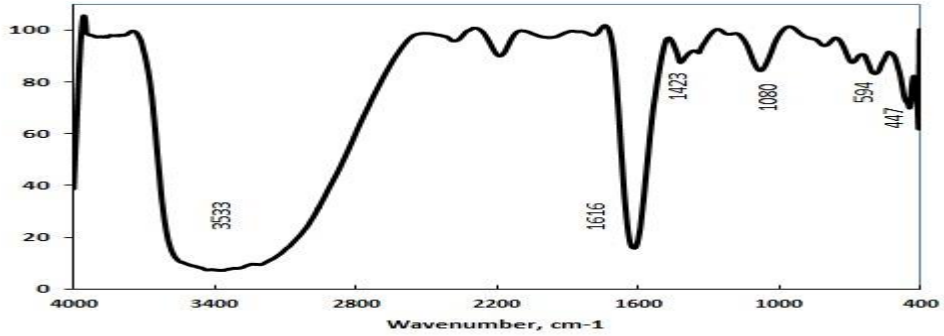

Figure 5. FT-IR of synthesized magnetite nanoparticles

3.4. Transmission electron microscopy (TEM) images

The morphology of magnetite nanoparticles was revealed by TEM technique. TEM image of green synthesized Fe3O4NPs showed that magnetite nanoparticles were in spherical shape, Figure6. Besides, a histogram of particle size distribution was drawn according to the size of 20 nanoparticles, Figure7. The average particle size was 20 nm with the standard deviation of 2 nm. The crystallite size of the synthesized Fe3O4NPs was found to be 18.8 nm from XRD analysis, which is in an agreement with the result obtained from the TEM that shows a size distribution between 11.0 and 20.0 nm. A few very small spherical objects can be observed from the image which might be due to the residue of *U. tomensota.*

Multidisciplinary Journal of Chemistry
Volume 11 Issue 1, January-March 2023
ISSN: 2995-4398
Impact Factor: 7.15
https://kloverjournals.org/journals/index.php/chem

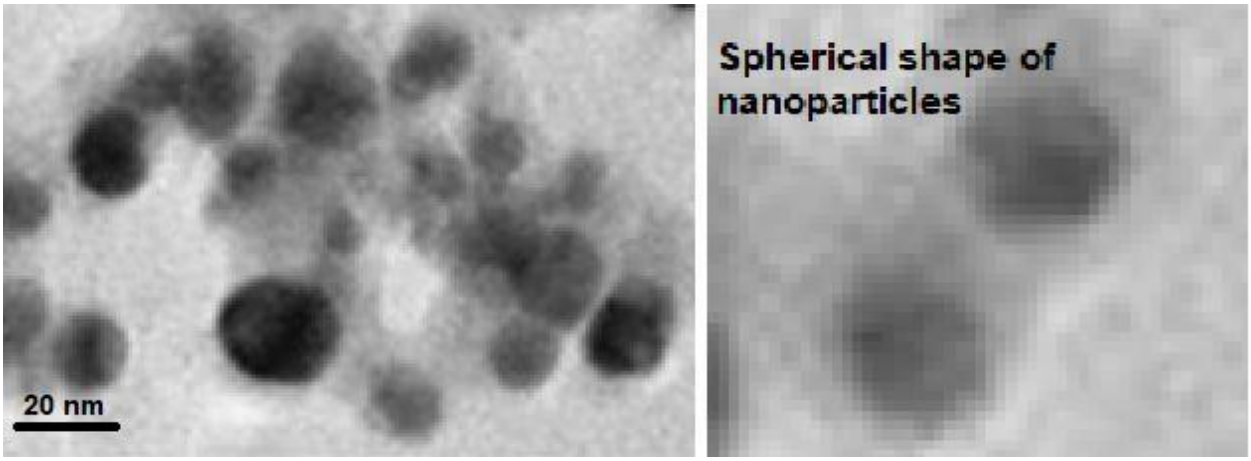

Figure 6. TEM images of synthesized magnetite nanoparticles

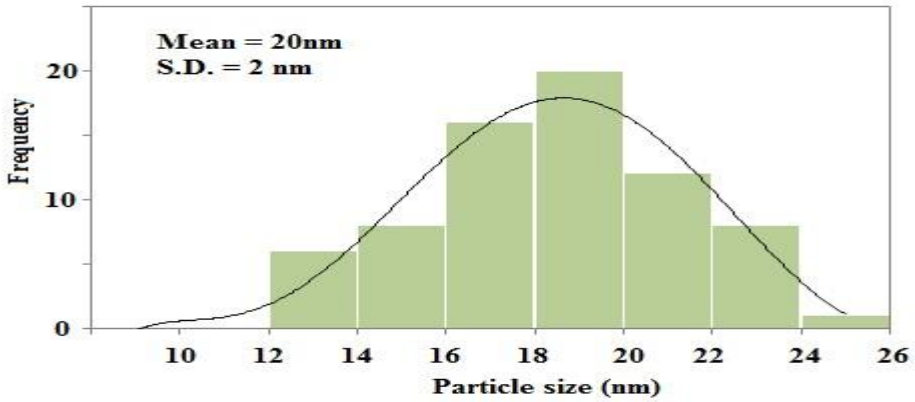

Figure 7. Histogram of particle size distribution of synthesized magnetite nanoparticles

3.5. Aphicidal effect of magnetite (Fe3O4 NPs) on the green peach aphid:

Toxicity was assessed through mortality percents and the data analysis for toxicity against early and late nymph instars constructed in Tables 1 and 2, respectively to compare between different concentrations of magnetite NPs used in bioassay experiments. On the both stage groups of GPA, the results showed increasing in mortality % with increase in concentrations and through time periods. For instance higher concentration (1000 ppm) showing higher mortality against both early (55%) and late (44%) nymphal instars after 24h compared with the other concentrations at the same period Tables 1 and 2. These percent of mortality increased with time to 86.2 and 73.8 for early and late stages, respectively after 72hr of treatment. There were significant differences among concentrations on their effects on the two categories of the GPA based on one way ANOVA analysis and LSD means separation. The means difference of (Fe3O4) NPs concentrations against early and late nymphal instars of the GPA were significant. Significantly levels were (0.13) and (0.037) for early and late instars, respectively **.**Also, mortality % of both categories of aphid treated with all concentrations were significantly higher than the two controls treatment. The effect of all concentrations against early and late nymphal instars were higher than the aqueous extract effect as represented in Tables (1 and 2) which means that the mortality of GPA was due to magnetite NPs effect rather than the extract effect. Plant extract effect was

Multidisciplinary Journal of Chemistry
Volume 11 Issue 1, January-March 2023
ISSN: 2995-4398
Impact Factor: 7.15
https://kloverjournals.org/journals/index.php/chem

closely to control effect and had no significant differences in their effect either on early or late nymph instars of GPA.

Table 1: Means of mortality percent (%) of early nymphal instars of the green peach aphid by different concentrations of magnetite (Fe3O4NPs) with time passing under lab conditions

Concentrations (ppm)	Mortality percent		
	24h	48h	72h
50	22.60 b ± 0.68	30.80 b ± 0.71	37.00 b ±0.78
100	27.00 b ± 0.55	34.80b ± 0.48	42.00 bc ± 1.14
200	32.80 c ± 0.92	43.20c ± 1.44	48.20 c ± 0.99
400	37.80 c ±0.88	47.60c ± 0.52	56.60d ± 0.94
600	48.60 d ± 0.94	57.40 d ± 0.79	68.00 e ± 0.88
800	51.20 de ± 1.31	62.20de ± 2.44	76.00 f ± 2.13
1000	55.00 e ± 0.82	76.80 e ± 2.23	86.20 g± 2.68
C*	2.6 a ± 0.54	5.00 a ± 0.98	6.40 a ± 1.47
C1**	2.4 a± 0.66	3.70 a ± 0.68	5.60 a ± 0.78

Means in the same column sharing the same small letter did not differ significantly using LSD test at 5% probability level.

C*: is the control No 1; using water alone.

C1** : the control No 2; using the aqueous extract alone.

Table.2: Means of mortality percent (%) of late nymph instars of the green peach aphid by different concentrations of Fe3O4NPs under lab conditions.

Concentration (ppm)	Mortality percent		
	24h	48h	72h
50	12.60 b ± 0.67	21.40 b± 1.030	25.80b ± .735
100	16.60 c ± 0.42	24.80 c± 490	29.60 c ± .980
200	23.20 d ± 0 .76	31.40 d± .678	36.20 d ± .735
400	27.40 e± 0.75	36.60 e± .245	45.40 e± .678
600	37.60 f± 0.56	46.00 f± .837	55.60 f± .600
800	40.40 g ± 1.03	53.40 g± 1.833	62.60 g± 1.887
1000	44.00 h ± 1.09	66.00 h± 2.098	73.80 h± 2.458
C*	3.2 a ± 1.24	5.00 a ± 1.09	6.20 a ± 1.48
C1**	2.9 a ± .66	5.20 a ± 0.58	6.80 a ± 0.95

Means in the same column sharing the same small letter did not differ significantly using LSD test at 5%

probability level.
C*: is the control No 1; using water alone.
C1** : the control No 2; using the aqueous extract alone.

Conclusion

In the present work, we first report an eco-friendly and simple method for synthesis of magnetite nanoparticles (Fe3O4) using *U. tomentosa* leaves aqueous extract. FTIR analysis of aqueous *U. tomentosa* extract indicated the presence of phyto-constituents such as amines, aldehydes, phenols, and alcohols, which were the surface active molecules stabilized the magnetite nanoparticles. XRD analysis reveals that the average size of the nanoparticles was found to be 20 nm which was calculated by Debye-Scherrer equation. FT-IR and XRD results corroborated the purity of the synthesized Fe3O4NPs. Green synthesized Fe3O4NPs was evaluated against green peach aphid showing a significant effective activity. The method of the present study offers several important advantageous features. First, the synthesis route is economical and environmentally friendly, because it involves inexpensive and non-toxic materials, and large scale synthesis.

Acknowledgments

Authors are thankful to the Royal Scientific Society and the University of Jordan for giving all facilities to carry out this research work.

Conflict of Interest

Authors declare that there is no conflict of interests regarding the publication of this manuscript

References

Angermann, A., Töpfer, J. (2008). Synthesis of magnetite nanoparticles by thermal decomposition of ferrous oxalate dihydrate. J. Mater. Sci. 43, 5123-5130.

Ahmed, M.J.K., ahmaruzzaman, M., Bordoloi, M.H. (2015). Novel Averrhoa carambola stabilized magnetite nanoparticles: a green synthesis route for the removal of chlorazol black E from wastewater. RSC Adv., 5, 74645-74655.

Awwad AM, Salman NM. (2012). A green and facile approach for synthesis of magnetite nanoparticles. J. nanosci. and Nanotechnol. 2, 208-213.

Cabrera, L., Gutierrez, S. (2008). Magnetite nanoparticles: Electrochemical Synthesis and characterization. Electrochimica Acta, 53, 3436-3441.

Chin, S.F., Pang, S.C., Tan, C.H. (2011). Green synthesis of magnetite nanoparticles via thermal decomposition method with controllable size and shape. J. Mater. Environ. Sci., 2, 299-302.

Das, A. K., Marwal, A., Verma, R. (2014). Bio-reductive synthesis and characterization of plant protein coated magnetite nanoparticles. Nano Hybrids 7, 69-86. de Carvalho, J. F., De Medeiros, S. N.,

Morales, M. A., Dantas, A. L., Carrico, A. S. (2013). Synthesis of magnetite nanoparticles by high energy ball milling. Appl. Surf. Sci., 275, 84-87.

Ge, S., Shi, X., Sun, K., Li, C., Uher, C., Baker, J. R., Banaszak, M. M. (2009). Facile hydrothermal synthesis of iron oxide nanoparticles with tunable magnetic properties. J. Physical Chemistry C., 113, 13593-13599.

Hou, Y., Yu, J., Gao, S. J. (2003). Solvothermal reduction synthesis and characterization of superparamagnetic magnetite nanoparticles. Mater. Chem., 13, 1983-1987.

Iwasaki, T., Mizutani, N., Watano, S., Yanagida, T., Kawai, T. (2012). Hydrothermal synthesis of magnetite nanoparticles *via* sequential formation of iron hydroxide precipitates. J. Exper. Nanosci. 7.

Karkuzhali, Yogamoorthi A. (2015). Biosynthesis of iron oxide nanoparticles using aqueous extract of *Jatropha gosspifolia* as source of reducing agent. International Journal of NanoScience and Nanotechnology 6, 46-55.

Latha1, N., M. Gowri, M. (2014). Bio synthesis and characterisation of Fe3O4 nanoparticles using *Caricaya papaya* leaves extract. International Journal of Science and Research 3, 1551-1556.

Liu, Z. L., Wang, X, Yao, K.L., Du, G.H., Lu, Q. H, Ding, Z. H.,Tao, J., Ning, Q., Luo, X. P., Tian, D.Y., Xi, D. (2004). Synthesis of magnetite nanoparticles in W/O microemulsion. J. Mater. Sci. 39, 2633-2639.

Mahdavi, M., Namvar, F., Bin Ahmad, M., Mohamad, R. (2013). Green biosynthesis and characterization of magnetic iron oxide (Fe3O4) nanoparticles using seaweed (*Sargass ummuticum*) aqueous extract. Molecules 18, 5954-5964.

Maheswari, K. C., P. S. Reddy, P. S. (2016). Green synthesis of magnetite nanoparticles through leaf extract of *Azadirach taindica*. J. Nanoscience and Technology 2, 189-191.

Maity, D., Yi, J., Ding, J., Xue , J. M. (2009). Synthesis of magnetite nanoparticles via a solvent-free thermal decomposition route. J. Magn. and Mag. Mater. 321, 1256-1259.

Ou, P., Xu, G., Xu, C., Zhang, Y., Hou, X., Han, G. (2010). Synthesis and characterization of magnetite nanoparticles by a simple solvothermal method.Mater. Sci., Poland 28, 817-822.

Petcharoen, K., Sirivat A. (2012). Synthesis and characterization of magnetite nanoparticles via chemical coprecipitation method.Mater. Sci. and Eng.: B, 177, 421-427.

Salem, N.M. Ahmad, L.A., Awwad, A.M. (2013). New route for synthesis magnetite nanoparticles from ferrous ions and pistachio leaf extract. J. nanoscience and Nanotechnology, 3, 48-51.

Senthil, M., Ramesh, C. (2012). Biogenic synthesis of Fe_3O_4 nanoparticles using *Tridaxprocumbens* leaf extract and its antibacterial activity on *Pseudomonas aeruginosa*. Digest Journal of Nanomaterials and Biostructures 7, 16551660.

Sun, S., Zeng, H. (2002). Size-controlled synthesis of magnetite nanoparticles, J. Am. Chem. Soc. 124, 8204-8205.

Valentin, V. M., Svetlana, S.M., Andrew, J. L., Olga, V.S., Anna, O. D., Igor, V.Y., Michael, E. T., Natalia, O. K. (2014). Biosynthesis of stable iron oxide nanoparticles in aqueous extracts of *Hordeum vulgare* and *Rumexacetosa* plants. Langmuir 30, 5982–5988.

Vega-Chacón, J., Picasso, G., Avilés-Félix, L., Jafelicci, Jr M. (2016). Influence of synthesis experimental parameters on the formation of magnetite nanoparticles prepared by polyol method. Advan. in Nat. Sci.: Nanosci. and Nanotechnol.7,015014

Venkateswarlu, S., Kumur, B. N., Prathima, B., Rao, Y. S., N.V.V. Jyothi, N. V. V. (2017). A novel green synthesis of Fe_3O_4 magnetic nanorods using *Punica granatum* rind extract and its application for removal of Pb(II) from aqueous environment. Arabian Journal of Chemistry 7.

Xu, J., Yang, H., Fu, W., Du, K., Sui, Y., Chen, J., Zeng, Y., Li, M., Zou, G. (2007). Preparation and magnetic properties of magnetite nanoparticles by sol-gel method. J. Magn. Magn. Mater. 309, 307-311.

Yew, Y.P., Shameli, K., Miyake, M., Kuwano, N., Khairudin, N.B., Mohamad, S., Lee, K. X. (2016). Green synthesis of magnetite (Fe_3O_4) nanoparticles using seaweed (Kappa phycusalvarezii) extract. Nanoscale Research Letters, **11**:276.